forests

MDPI

Article

Douglas Fir Multiproxy Tree-Ring Data Glimpse MIS 5 Environment in the U.S. Pacific Northwest

Irina P. Panyushkina [1,*], Steven W. Leavitt [1], David M. Meko [1], Bryan A. Black [1], A. J. Timothy Jull [2], Peter Van de Water [3], Joe Squire [4] and Nicholas R. Testa [5]

[1] Laboratory of Tree-Ring Research, University of Arizona, Tucson, AZ 85721, USA
[2] Department of Geosciences, University of Arizona, Tucson, AZ 85721, USA
[3] Department of Earth and Environmental Sciences, California State University, Fresno, CA 93740, USA
[4] CDR Emergency Management, 2025 Vista Ave SE, Salem, OR 97302, USA
[5] Oregon Department of Transportation, Corvallis, OR 97301, USA
* Correspondence: ipanyush@arizona.edu

Abstract: Proxy records from the late Quaternary help in understanding climate variability on extended time scales. An ancient landslide deposit in Oregon U.S.A. preserved large logs from Douglas fir trees (*Pseudotsuga menziesii* (Mirb.) Franco) and afforded an opportunity to explore the response of tree growth to climate on annual and decadal scales. High-precision radiocarbon dating indicates an age exceeding 63 ka, i.e., the trees grew within the generally cool Marine Isotope Stage 5 (MIS 5), likely during a warmer interval optimal for Douglas fir establishment. This would include the prolonged warm MIS 5e (ca. 110–130 ka), corresponding approximately to the Eemian interglacial, which was warm like the current Holocene interglacial. A 297-year tree-ring width chronology from 12 Douglas fir logs and 227-year tree-ring $\delta^{13}C$ and $\delta^{18}O$ records are analyzed with spectral and wavelet analysis. Variance of the ancient rings is consistent with modern Douglas fir growth sensitive to moisture and ecological disturbances. Spectra of ancient and modern chronologies are dominated by low frequencies with significant spectral peaks appearing at high frequencies (2.1–4 years) and cyclic behavior transient over centuries. It is conceivable that the O-isotopes track moisture and that C-isotopes track temperature or sunlight. The findings illustrate the challenges in assessing the response of ancient tree-ring properties to late Quaternary climate variability.

Keywords: tree-ring proxy; Eemian interglacial; climate variability; stable isotopes; wood macrofossils; late Quaternary; *Pseudotsuga* Carrière

Citation: Panyushkina, I.P.; Leavitt, S.W.; Meko, D.M.; Black, B.A.; Jull, A.J.T.; Van de Water, P.; Squire, J.; Testa, N.R. Douglas Fir Multiproxy Tree-Ring Data Glimpse MIS 5 Environment in the U.S. Pacific Northwest. *Forests* **2022**, *13*, 2161. https://doi.org/10.3390/f13122161

Academic Editors: Olga Churakova (Sidorova) and Marco M. Lehmann

Received: 21 November 2022
Accepted: 13 December 2022
Published: 16 December 2022

1. Introduction

Coupled ocean–atmosphere simulations of the Last Glacial Maximum (LGM, ca. 30,000 to 20,000 years ago) climate employs orbital time scales to describe sea level and glacial/interglacial cycles, monsoon variability, interhemispheric connections, and insolation forcing [1]. LGM atmospheric circulation was strongly affected by glacial ice sheets over northern mid-latitudes, which have altered the thermohaline circulation as well. Such circulation changes played a key role in determining regional climate change patterns and vegetation. Along the west coast of the Americas, an equatorward shift in the westerlies in both hemispheres during the LGM led to conditions that are relatively wetter and colder than present in the region [2]. Many lines of proxy evidence suggest that the frequency of interannual extreme events and decadal variability are modulated by the El Niño Southern Oscillation (ENSO) teleconnections, although the global imprint of ENSO was very different during the LGM and its effects have not been identified with great precision [3,4]. More finely resolved proxy records like tree rings are essential to understanding the patterns of LGM (and Late Quaternary more generally, i.e., during the end of the last 2.5 million years) climate change on various time scales and their relationships to ENSO and other teleconnected climate processes.

In this study we aimed to develop well-replicated multi-parameter chronologies from Douglas fir (*Pseudotsuga menziesii* (Mirb.) Franco) subfossil wood associated with U.S. Pacific coastal environments and investigate tree-ring proxies as indicators of late Pleistocene climate variability. Douglas fir is currently a widespread tree species in North America and occurs in two varieties (Figure 1). Coast Douglas fir (*Pseudotsuga menziesii* var. *menziesii* (Mirb.) Franco) has a natural range that extends along the Pacific coast from California up into British Columbia, while Rocky Mountain Douglas fir (*Pseudotsuga menziesii* var. *glauca* (Mayr) Franco) occurs inland from western Canada through Arizona and New Mexico and into Mexico [5]. Brubaker (1991) [6] proposed that evidence from climate modeling indicates western Oregon was probably too cold and dry to support the large-scale survival of Douglas fir forests during the LGM. However, Gugger and Sugita (2010) [7] assembled all available Douglas fir pollen and macrofossil records to infer both species' geographic distributions through time and the rate of migrations in the late Quaternary. This evidence indicates the presence of coast Douglas fir in western Oregon and Washington (west of the Cascade Range) back to 40,000 ^{14}C y BP. The presence of glaciers during the late Pleistocene (40,000 to 21,000 y BP) might have inhibited and fragmented Douglas fir distribution northward into Washington, but Gugger and Sugita (2010) [7] proposed that a more "consistent" coastal climate, as modelled by Bartlein et al. (1998) [8] plus the generally lower "topographic complexity" of the coastal areas, may have provided favorable environments for the distribution of coast Douglas fir from California north to Washington, at least during the period since the LGM (Figure 1). Paleoclimate modelling intercomparisons generally support these conclusions and provide greater temporal resolution of the climate variability throughout the LGM [1,4].

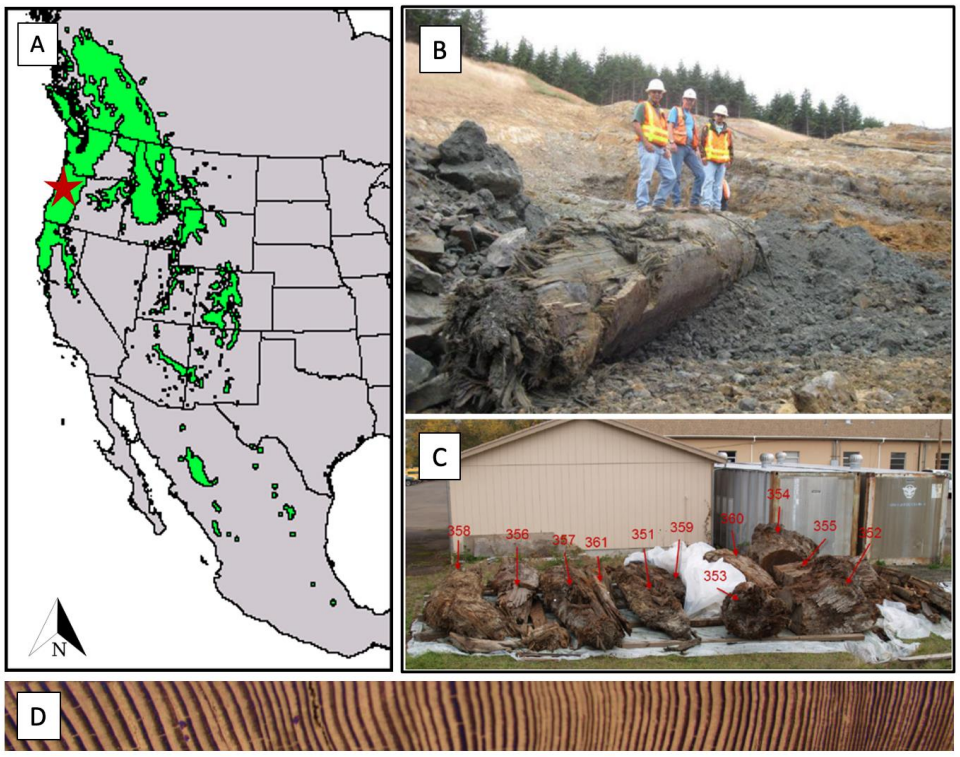

Figure 1. Map of modern Douglas fir distribution in North America (after Little, 1971) [9] (**A**); the red star marks the location of the landslide in the state of Oregon whose southern border is ca. 600 km long). Field photo of ancient Douglas fir trunk preserved in a landslide deposit along US Highway 20 in Oregon (**B**). Assemblage of Douglas fir logs retrieved from the landslide deposit stored in the Oregon Department of Transportation yard in Corvallis, Oregon (**C**); photo credit P. Van de Water). Numbers identify the tree-ring specimens subsampled for this study. Image of tree rings from one of the Douglas fir logs (**D**).

Modern Douglas fir wood has been extensively used in the dendrochronology of western North America to develop ring-width chronologies for dating and climate reconstruction from Mexico to Canada (e.g., [10–14]). Old-growth coast Douglas fir trees in Oregon may reach 400–500 years in age, and according to the Klamath Inventory and Monitoring Network (2017) [15], old coast Douglas fir trees may reach a height of 76 m, with diameter of 1.5–2.1 m, and the tallest individuals measure over 90 m with a diameter of 4.5–5.5 m. Tappeiner et al. (1997) [16] considers Douglas fir stand density (trees/ha) in western Oregon to be generally low but highly variable. Our case study employs subfossil logs from ancient landslides identified by geotechnical reconnaissance during the realign-

Modern Douglas fir wood has been extensively used in the dendrochronology of western North America to develop ring-width chronologies for dating and climate reconstruction from Mexico to Canada (e.g., [10–14]). Old-growth coast Douglas fir trees in Oregon may reach 400–500 years in age, and according to the Klamath Inventory and Monitoring Network (2017) [15], old coast Douglas fir trees may reach a height of 76 m, with diameter of 1.5–2.1 m, and the tallest individuals measure over 90 m with a diameter of 4.5–5.5 m. Tappeiner et al. (1997) [16] considers Douglas fir stand density (trees/ha) in western Oregon to be generally low but highly variable. Our case study employs subfossil logs from ancient landslides identified by geotechnical reconnaissance during the realignment of U.S. Highway 20 from Corvallis to Newport, Oregon, at ca. 45° N latitude conducted in the late 1980s and early 1990s. Paleo-landslides ranging from 5 to 21 hectares were found during this preliminary geological investigation. Further investigations identified additional large landslide complexes along with 15 local slumps and debris flows. LIDAR was used to map more than one hundred landslide landforms within the project right-of-way [17]. During initial construction, additional information was gathered, which included field mapping, subsurface exploration, and the radiocarbon dating of subsurface organic deposits. The realignment of the Eddyville–Pioneer Mountain section of Highway 20 involved excavations to stabilize the hillslope and roadbed [18], and during the 2008–2009 construction phase, excavation unearthed large Douglas fir logs near Eddyville, Oregon. A dozen tree trunks entombed in one of the ancient landslides were recovered in 2008 (Figure 1). The Oregon Department of Transportation (ODOT) recognized their potential importance and took steps to conserve them during the excavation process and preserve them afterward. The largest individual tree bole in the recovered samples measures greater than 1.2 m in diameter. Approximately one-third of the recovered trees appear to be wholly intact, whereas the others comprise significant portions of the original large trunks. The landslide deposits also contained organic and peaty soil and sediments containing plant and animal macrofossils from which seeds and a Douglas fir cone were recovered. This paper explores the potential of tree-ring width and isotopic records from the coastal ancient landslide for the assessment of late Pleistocene climate conditions and variability.

2. Methods

2.1. Dendrochronology

Large cross-sections of the recovered trunks were cut with a chainsaw by ODOT and conveyed to the University of Arizona in a 5-ton shipment in October 2010, and samples were prepared and dated in 2011. The wood shows excellent preservation of latewood rings, but earlywood shows some degradation with a high percentage of incomplete "ghost tracheids". At the Laboratory of Tree-Ring Research (LTRR), the samples were cut with a band saw to manageable sizes containing a complete radius of tree rings from pith to bark. Two radial subsamples from each cross-section were subsequently sanded with progressively finer grit to produce distinct and clear ring surfaces. Ring widths were measured to 0.01 mm on a LINTAB stage system (Rinntech-Metriwerk GmbH & Co. KG, Heidelberg, Germany). The tree-ring series were crossdated visually through the plotting of tree-ring width measurements, then the tree-ring positions were checked with correlations in the program COFECHA [19]. Table S1 in Supplementary Materials summarizes the tree-ring statistics of thirteen crossdated series. The tree-ring width chronology was computed using program ARSTAN [20]. The crossdated series were detrended with negative exponential curves. The individual detrended series were combined into a standard chronology using a bi-weight robust mean.

2.2. Stable Isotopes

Crossdating results enabled the pooling of contemporaneous rings from four trees for isotope analysis in 2012–2014. The first two decades were not analyzed to minimize possible juvenile growth-related isotopic effects [21]. Tree rings from two radii of each of four trees were separated and pooled together for most years; except that ca. every 10 years,

the rings of the trees were maintained separately to characterize any differences in absolute values and patterns among trees and for a quantitative estimate of isotopic variance among trees. The rings were then ground to 20-mesh in a Wiley Mini-Mill (Thomas Scientific Inc., Swedesboro, NJ, USA). The milled wood samples were converted to holocellulose and then to α-cellulose using the Jayme–Wise oxidation method [22,23] through a procedure using the batch processing of samples in which individual samples were contained in the compartments of commercial digestion pouches (ANKOM Technology, Boston, MA, USA) during chemical processing. Extractives in the wood were first removed with organic solvents toluene/ethanol and then ethanol in a soxhlet extraction apparatus, followed by boiling in deionized water. Lignin was removed by oxidation in an acetic-acid-acidified, sodium chlorite aqueous solution at 70 °C, rinsed thoroughly in deionized water, and then dried at 70 °C. These holocellulose samples were treated with 17% NaOH to isolate α-cellulose [24]. Samples for both isotopes were analyzed on a Finnigan Delta-Plus mass spectrometer in flow-through mode at the Environmental Isotope Laboratory, University of Arizona. Working standards of known isotopic composition were run every three to six samples to monitor mass-spectrometer reproducibility (analytical precision) and accuracy. One split of α-cellulose was combusted to CO_2 at 1030 °C in an elemental analyzer, with combustion products carried by a helium carrier gas and separated in a gas chromatograph, after which the gas stream was introduced into the mass spectrometer for $\delta^{13}C$ analysis. One split of α-cellulose was pyrolized/combusted to CO at 1350 °C, separated by gas chromatography, and admitted into the mass spectrometer for $\delta^{18}O$ analysis. Isotopic results in permil (‰) units are reported with respect to the Vienna Pee Dee Belemnite (VPDB) standard for $\delta^{13}C$ and the Vienna Standard Mean Ocean Water (VSMOW) standard for $\delta^{18}O$. Over the course of sample runs for this project, repeated $\delta^{13}C$ analysis of an acetylnide working standard indicated a precision (mean of standard deviation) of 0.04‰, and repeated analysis of an Aldrich cellulose lab standard yielded a precision (mean of standard deviation) of 0.19‰. Repeated $\delta^{18}O$ analysis of Sigma cellulose and benzoic acid working standards gave a precision (mean of standard deviation) of 0.29‰ and 0.27‰, respectively. Additionally, replicate analysis of the pooled samples ca. every 10 years yielded a mean $\delta^{13}C$ difference between replicates of 0.01‰ (std dev = 0.19‰) for 29 rings and a mean $\delta^{18}O$ difference between replicates of 0.15‰ (std dev = 0.91‰) for 25 rings. Removal of the most extreme outlier difference of 3.33‰ for $\delta^{18}O$ (more than twice as large as any other difference) resulted in a mean difference between replicates of 0.01‰ (std dev = 0.64‰) for 24 rings.

2.3. Spectral Analysis

Variations of tree-ring width chronology and isotope series averaged per isotope were summarized by smoothed periodogram spectral analysis [25] and wavelet analysis [26,27]. For spectral analysis, the raw periodogram of a padded (to next highest power of two) and tapered (5% of each end) time series were smoothed with a succession of equal-length Daniell filters to achieve a target bandwidth of the spectral estimate. Confidence intervals for spectral estimates were not adjusted for multiple comparisons (e.g., no Bonferroni adjustment). For wavelet analysis, the Morlet wavelet (6.0/6) was applied to summarize changes in the amplitude of oscillations as a function of time and frequency, which were displayed in color maps of the continuous wavelet transform (CWT; [27]). CWT plots were paired with plots of the time series smoothed with a Hamming [28] low-pass finite impulse response filter designed to emphasize decadal-and-longer wavelengths. Spectral and CWT analysis were done with MATLAB software (Version 9.4, Natick, MA, USA).

Cross-wavelet analysis [27] was applied to test the coherency of ring width index and isotope averaged values. Coherency is analogous to correlation as a function of frequency. Significant levels of coherency were defined with Monte Carlo testing [27]. Linkage of ancient ring cyclicity to climate is assessed via a comparison of spectral properties of modern Douglas fir chronologies from the Coastal Range of Oregon, which show diverse influences from climate forcing and ecological disturbances [29,30].

2.4. Radiocarbon Dating

The initial age determination of the logs was done at the University of Arizona AMS (Accelerator Mass Spectrometer) dating laboratory in December 2009 on subsamples from 10 of the logs, one of which (specimen #355, Supplementary Materials Table S1) was subsampled on the inside and outside for separate analysis. The samples were broken into small pieces and given a standard ABA (acid–base–acid) pretreatment, in which samples were successively soaked at 70 °C in an HCl solution overnight, a 70 °C NaOH solution overnight, and a second 70 °C HCl solution overnight, with rinsing in deionized water after each treatment [31]. The pretreated samples were combusted to CO_2 and converted to graphite for AMS targets [32]. Maximum measures were taken during processing and analysis to push back the dating limit, such as using low-blank vacuum lines for handling sample gases [33] and extended periods of AMS measurement. A correction for isotopic fractionation was applied based on the stable-carbon isotope composition of the sample. Table S3 of Supplementary Materials shows the Arizona AMS measurements, but those ages unfortunately exceeded the maximum detection limit attainable with the Arizona AMS equipment and protocols and therefore could only be reported as ca. greater than 52,000 y BP.

The second series of AMS radiocarbon measurements were done in 2014 at the Radiocarbon Dating Laboratory, University of Waikato, New Zealand, which specialized in ultra-high-precision radiocarbon dating and long decay counting. We resampled three Douglas fir log samples and ground ca. 160 g of wood subsamples containing 10 years of rings from each of three trees (specimens #351, 354, 358, Table S1) finely enough to pass through a 20-mesh sieve. These were processed via duplicate analysis (ca. 80 g per duplicate) to achieve the highest precision, and furthermore they were processed at Waikato along with two ancient kauri blank samples (ca. 160 ka) to assure confidence in the processing and to establish pretreatment backgrounds. Soluble wood extractives were removed by dissolution in acetone and then water. Alpha-cellulose was isolated by first removing lignin and hemicelluloses with six treatments with 6 mL of concentrated HCl and 15 g $NaClO_2$ (sodium chlorite) and rinsing with deionized water. This was followed by 1000 mL 5% w/v NaOH added for 30 min under N_2 gas and then rinsing with deionized water. Finally, the cellulose samples were reacted with 5% HCl, filtered, rinsed, and dried. The alpha-cellulose was converted to benzene [34] that sat undisturbed for ca. 30 days to ensure there was no radon present before liquid scintillation counting began. The counting was done for ca. 2 weeks per sample. Each measured result is reported as conventional age or percent modern carbon (pMC) following Stuiver and Polach (1977) [35]. This is based on the Libby half-life of 5568 years, with correction for isotopic fractionation applied. Because these are lower limits to the age, the ages are calculated according to the convention of Stuiver and Polach (1977) [35] for limit ages.

3. Results and Discussion

3.1. Tree-Ring Multi-Parameter Records

The microscopic inspection of wood anatomy for 11 recovered trees was done at the USDA Forest Products Lab, Madison, WI, and revealed all to be Douglas fir (*Pseudotsuga*), but taxonomy could not be differentiated at the species level. All sampled logs from the landslide tree cohort were successfully crossdated into a 297-year ring width chronology (Figure 2a) with 0.58 serial correlation and standard deviation 0.20. The sample depth of more than five trees covers 295 years of the ring index record, whose sufficient length and sample size support meaningful insights into the interannual, decadal, and multidecadal variability in tree growth that possibly responds to climate.

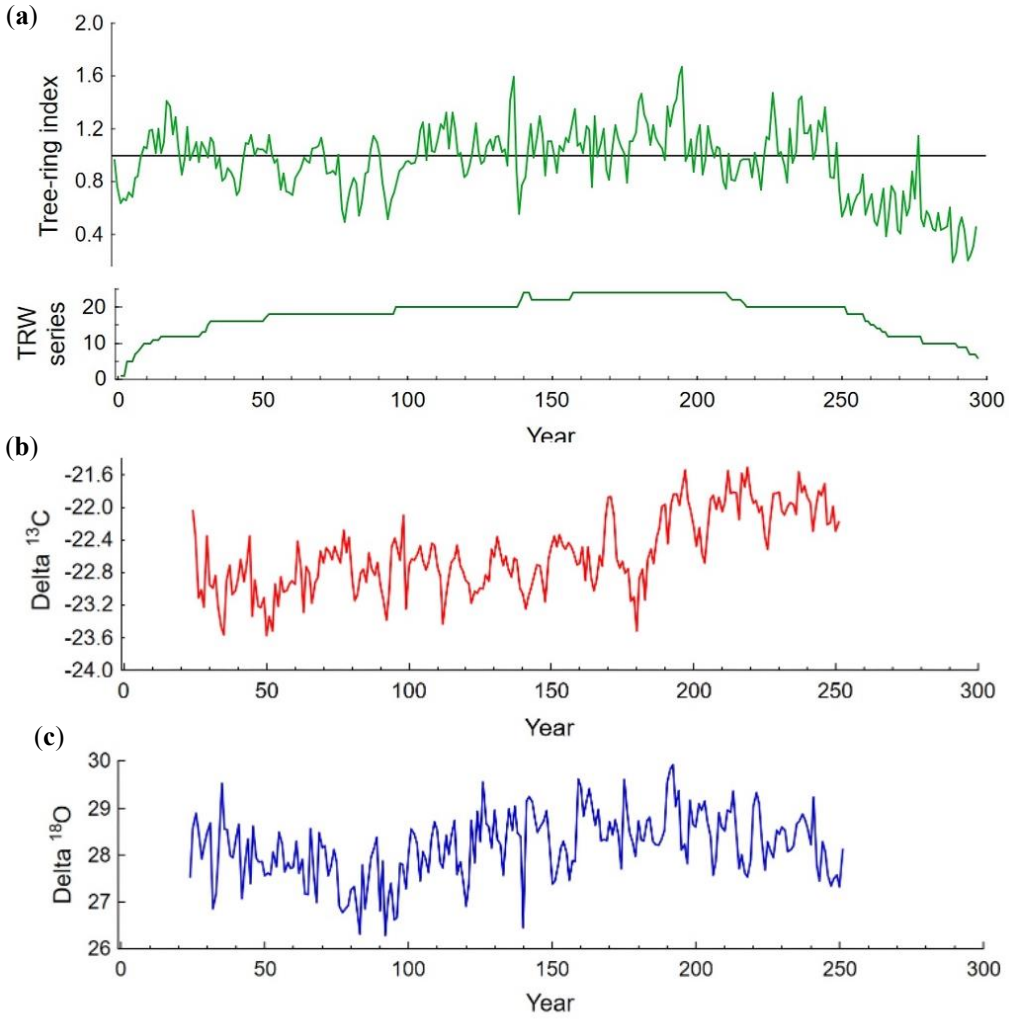

Figure 2. Tree-ring chronologies developed from width (**a**), $\delta^{13}C$ (**b**), and $\delta^{18}O$ (**c**) of the tree rings of Douglas fir found in the ancient landslide. The panel below the ring width chronology (**a**) indicates the number of tree-ring series included into the chronology.

In addition to the 297-year ring width chronology, $\delta^{13}C$ and $\delta^{18}O$ records were developed from four of the longest-lived trees by two methods: (1) pooling rings prior to analysis for most years and (2) analyzing rings separately and then averaging values for ca. 10% of years. Sampling four to six trees has been shown to produce isotope chronologies representative of a site in many environments [36,37]. Supplementary Materials include Figure S1 isotopic composition of pooled samples and isotopic composition of the trees analyzed separately every decade. The isotope records are 227 years long and span from Year 24 to Year 251 of the ring width chronology (Figure 2b,c). Some additional C isotope measurements were made for years after 250, but only from one tree, so there is less confidence in them. For the years when all four trees were analyzed separately, the greatest range for $\delta^{18}O$ values was 3.58‰, and the smallest was 0.28‰ (average range = 1.65‰, standard deviation (SD) = 0.80‰). The average standard deviation among the trees analyzed separately was 0.73‰. As for $\delta^{13}C$ in the period with all four trees analyzed separately, the greatest range was 2.49‰, and the smallest was 0.67‰ (average range of 1.50‰, SD = 0.57‰). A second measure is standard deviation among the trees analyzed separately, which averages 0.66‰. Both isotopic records can be considered usable for exploring common environmental influences on $\delta^{13}C$ and $\delta^{18}O$. The $\delta^{13}C$ mean of the studied intervals is −22.56‰, and the $\delta^{18}O$ mean is 28.11‰. $\delta^{13}C$ was positively correlated with $\delta^{18}O$, r = 0.18 ($p < 0.01$) (Table 1), although part of this relationship may be related to the upward trend exhibited by both

isotopes. Correlation of first differences was used to eliminate the influence of trends, and the relationship between the isotope series was not significant, r = 0.01 (p = 0.89). The tree-ring width chronology correlates significantly only with the $\delta^{18}O$ chronology, although the $\delta^{18}O$ record correlates with both other chronologies (Table 1).

Table 1. Correlation between ancient Douglas fir ring chronologies for the common interval of 228 years. Asterisk marks a significant correlation at $p < 0.005$.

Parameter	TRW (Tree-Ring Width Parameter)	$\delta^{13}C$	Standard Deviation
TRW			0.19
$\delta^{13}C$	0.10		0.47
$\delta^{18}O$	0.35 *	0.18 *	0.69

3.2. Interpretation of ^{14}C Dating

Age determination of the wood yielded ^{14}C ages beyond the current limits of radiocarbon dating. ODOT obtained an uncalibrated radiocarbon age on the first recovered tree trunk of >40,000 ^{14}C y (Beta-247622) and a subsequent sample dated >45,000 (Beta-264255). If the absolute age was close to these, the trees would have been growing during the generally cold Marine Isotope Stage 3 (MIS 3, ca. 60 to 27 ka, based on climate periods identified in the record of oxygen isotope variations in marine sediment cores) [38], perhaps more likely during one of the repeated abrupt but brief Dansgaard–Oeschger warm excursions [39] during MIS 3. The application of best-practice radiocarbon techniques to ancient organic matter near the limits of dating pushes the age to >52,000 ^{14}C y BP from the University of Arizona AMS facility (Table S3). Subsequent state-of-art, ultra-high-precision liquid scintillation dating at the University of Waikato pushed dating back 10,000 ^{14}C years, determining that ages exceeded ca. 62,000 ^{14}C y BP. Table 2 shows the ^{14}C measurements from this high-precision liquid scintillation counting. This indicates that some landslides in this area are older than 62,000 years.

Table 2. Radiocarbon dating results from high-precision liquid scintillation counting at University of Waikato, NZ. Notice that the ages actually reflect the background levels achieved during dating.

Tree	10-Year Ring Group	Sample ID	^{14}C pMC with Error	Minimum Age ^{14}C y BP	Average Age ^{14}C y BP
#351A	230–239	Wk-38751	0.004 ± 0.019	62,440	>62,255
#351B		Wk-38794	0.006 ± 0.019	62,070	
#354A	130–139	Wk-38752	−0.021 ± 0.020	62,500	>62,315
#354B		Wk-38795	−0.020 ± 0.022	62,130	
#358A	190–199	Wk-38753	−0.010 ± 0.020	62,800	>63,430
#358B		Wk-38796	0.000 ± 0.017	64,060	

The true absolute age of these trees is not clearly established with ^{14}C dating but might be constrained by other age proxies from the area. Buried forests dating from recent to ancient have been found along the Oregon coast [40]. The work of Smyth et al. (2005) [41] describes a particular deposit of trees buried by a landslide adjacent to U.S. Highway 101 in coastal Oregon with radiocarbon ages greater than 50,000 y BP. These trees were thought to be spruce, and geological evidence suggests the trees grew after 80,000 BP when a wave-cut platform was formed, above which the paleosoils and tree trunks are located.

Unfortunately, we do not have any such geological evidence to constrain the maximum age of the trees. However, if the age is 63,000 y BP, the trees would be in Marine Isotope Stage 4 (ca. 72,000 to 58,000 years ago [42,43], during which conditions would be cold according to NGRIP oxygen isotopes [39]. It seems more likely that that the trees were growing in the Eemian interglacial ca. 130,000 to 115,000 years ago, whose climate was like modern Holocene conditions. The Eemian is approximately coincident with the

MIS 5e substage (ca. 134,000 to 119,000 years ago) of MIS 5 [42–44]. After the Eemian, conditions progressively cooled through the end of MIS 5 ca. 70,000 years ago. Brief warmer intervals during the MIS 5 cooling might have been favorable to establishing and supporting Douglas fir forests in Oregon, but the Eemian/MIS 5e period would have been a longer phase of sustained favorable conditions for the trees. The age of the trees exceeding 100,000 years would provide evidence of an even longer period of landslide activity in this area. Employing high-precision radiocarbon dating to establish an age of such old trees preserved in the landslide provides more certainty when cross-referenced against other age-relevant factors.

3.3. Stable Isotopes

Because this is an ancient floating chronology, we cannot perform standard dendroclimatology, which compares climate data with ring widths and isotopes to establish statistical relationships. Ring widths of inland and coastal Douglas fir have been found to correlate with moisture and drought metrics (e.g., precipitation, standardized precipitation index, vapor pressure deficit) [45–48]. Generally, tree-ring carbon isotopes are strongly influenced by the processes of photosynthesis and stomatal conductance, which in turn are frequently related to moisture availability (e.g., soil moisture, precipitation, vapor pressure deficit) but also sometimes to insolation (affecting photosynthesis) and temperature when moisture is not limiting [36]. Tree-ring oxygen isotopes are also often found to strongly relate to moisture (e.g., precipitation, relative humidity, vapor pressure deficit) contributing to the evaporative isotopic enrichment of water in the leaf but also to temperature, influencing the isotope composition of atmospheric source water [49].

Several studies have specifically examined the isotopic composition of modern Douglas fir tree rings, particularly with respect to ecophysiology, with vapor pressure deficit (VPD) seeming to be a dominant influence on both isotopes. Panek and Waring (1997) [50] examined Douglas fir tree rings along a gradient from coastal to inland and found that tree-ring $\delta^{13}C$ was significantly related to VPD and the ratio of modeled transpiration to potential transpiration. Levesque et al. (2013) [51] examined ring width (total, earlywood, and latewood) and both $\delta^{13}C$ and $\delta^{18}O$ in the tree rings of five primary European timber species at xeric and mesic sites to assess the potential performance of the species under warmer–drier future conditions. Although spruce and larch trees were inferred to be the most threatened by such climate change, coast Douglas fir at both xeric and mesic sites showed strong negative relationships for earlywood and latewood $\delta^{13}C$ with soil moisture deficit (SMD), more so for spring–summer SMD at the xeric site and summer SMD at the mesic site. Correlations of $\delta^{18}O$ with SMD were not as strong, but the strongest at the xeric site was earlywood $\delta^{18}O$ with May SWD and earlywood $\delta^{18}O$ with April–May–June SWD at the mesic site. Roden et al. (2005) [52] analyzed $\delta^{13}C$ and $\delta^{18}O$ of the tree rings of 12-year-old coast Douglas fir in Oregon and found variations in $\delta^{18}O$ values associated with VPD, which indicate their potential as a proxy for humidity and site water balance, but the signal for $\delta^{13}C$ was less certain because of the addition of N fertilizers to the plantation where the trees were growing. Barnard et al. (2012) [53] also analyzed $\delta^{13}C$ and $\delta^{18}O$ in the 2000–2007 tree rings of coast Douglas fir tree rings in Oregon and found that the isotopes covary related to relative humidity influencing stomatal conductance and evaporative demand, with stronger relationships exhibited by the more dominant trees.

Interestingly, another study using tree-ring isotopes of coastal Douglas fir regards a fungal disease known as Swiss needle cast, which causes leaf chlorosis and premature needle loss [54,55]. Changes in ring growth and $\delta^{13}C$ at a coast Douglas fir site were interpreted as resulting from a reduction in stomatal conductance and rates of photosynthesis caused by a decline in stomatal function [54]. At both the coast and inland Douglas fir sites, summer VPD was the primary environmental parameter influencing growth and both $\delta^{13}C$ and $\delta^{18}O$. Lee et al. [55] found synchronous growth reduction from disease in modern coastal and inland Douglas fir trees with a periodicity of 25–30 years, which correlated with winter and summer temperatures and summer precipitation, consistent with elevated

preted as resulting from a reduction in stomatal conductance and rates of photosynthesis caused by a decline in stomatal function [54]. At both the coast and inland Douglas fir sites, summer VPD was the primary environmental parameter influencing growth and both $\delta^{13}C$ and $\delta^{18}O$. Lee et al. [55] found synchronous growth reduction from disease in modern coastal and inland Douglas fir trees with a periodicity of 25–30 years, which correlated with winter and summer temperatures and summer precipitation, consistent with elevated tree-ring $\delta^{13}C$. Lee et al. [55] then analyzed two trees from the ancient coast Douglas fir collection and 20 years in the subject of this paper. They found periodicities of 7.5 years in one tree and 20 years in the other, and non-synchronous growth between the two trees suggested that they have been more influenced by non-climatic factors. Furthermore, their microscopic examination of Douglas fir needle from the landslide deposit revealed apparent fungal pseudothecia fruiting bodies clogging some of the needle stomata. Observations by one of us with experience in modern Oregon coast Douglas fir tree-ring chronologies (B.B.) led us to believe that the influence of Swiss needle cast would be more likely to influence the growth of trees subject to fog immediately adjacent to the coast than to our trees ca. 20 km inland.

3.4. Spectral Properties of the Tree-Ring Records

Spectral analysis of the ancient tree-ring records exposed big differences in the periodicity of the common variance stirring in the tree-ring width and isotopic records of MIS5 Douglas fir. Strong high-frequency variability at 2.9–4 yr bandwidth are notable in the tree-ring width and $\delta^{13}C$ chronologies (Figure 3). Low-frequency variance occurs only in the tree-ring width chronology. The $\delta^{18}O$ chronologies of Douglas fir do not retain any significant peaks. The lack of correspondence between the spectra of various tree-ring parameters suggest that their variability could be attributed to different climatic or non-climatic factors.

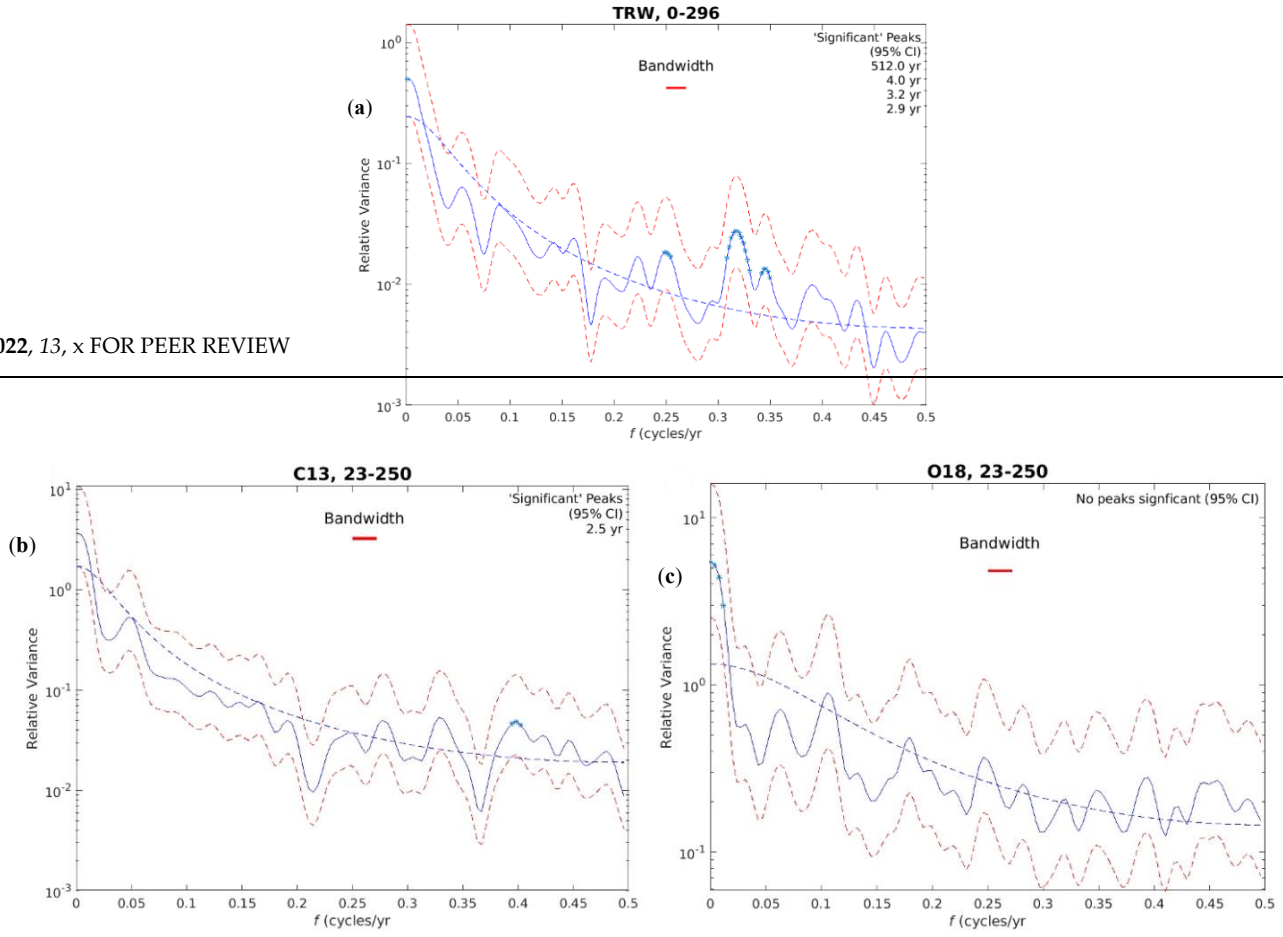

Figure 3. Spectrum of (**a**) ring-width, (**b**) $\delta^{13}C$, and (**c**) $\delta^{18}O$ chronologies of Douglas fir found in the ancient landslide in Oregon Coastal Range. Significant spectral peaks relative to red noise are listed at the top right. Red bar labeled "Bandwidth" describes the effective range of frequencies to which a given spectral estimate applies. Dashed line is the theoretical red noise spectrum. Analysis by smoothed periodogram method, as described in the Methods.

Wavelet analysis indicates that any cyclic behavior is transient in the ancient tree rings rather than persistent over centuries (Figure 4). Moreover, wavelets of ancient, as well as modern, chronologies of Douglas fir from the Coastal Oregon Range are dominated by low frequencies, but significant spectral peaks relative to red noise often appear

Wavelet analysis indicates that any cyclic behavior is transient in the ancient tree rings rather than persistent over centuries (Figure 4). Moreover, wavelets of ancient, as well as modern, chronologies of Douglas fir from the Coastal Oregon Range are dominated by low frequencies, but significant spectral peaks relative to red noise often appear at high frequencies, for example at wavelengths 2–4 years (Figures 4 and S2). The wavelet of the $\delta^{18}O$ record retains 8–16 years and very much resembles the wavelets of modern tree-ring widths, which respond to moisture variability [29,30]. Interestingly, spectral analysis of an ancient floating baldcypress tree-ring chronology from the eastern U.S., believed to also date to the last interglacial period, exhibits significant periodicity at 2.9, 5.7, 7.9, 17.5, and 52.0 years, which Stahle et al. (2012) [56] attribute to forcing by ocean–atmospheric climate modes in both the Pacific and Atlantic.

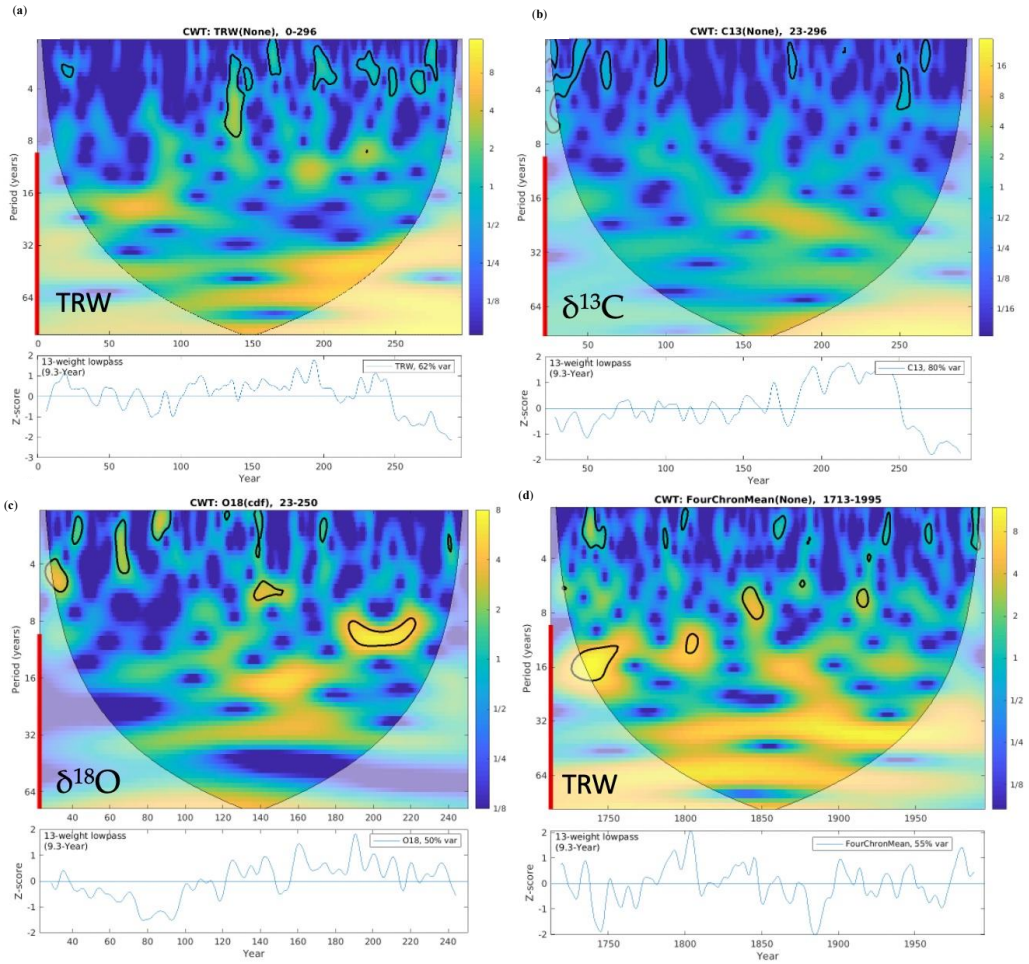

Figure 4. Continuous wavelet transforms (CWT) and smoothed plots of tree-ring time series. (**a**) Ring-width index chronology, floating, 297 years, for Douglas fir from an ancient landslide in Oregon Coastal Range, ca. 62,000 years ago. (**b**) $\delta^{13}C$ from a 228-year sequence of rings from the same wood samples. (**c**) $\delta^{18}O$ from the same rings as $\delta^{13}C$. (**d**) Ring-width index of the average of four modern Douglas fir chronologies from central Oregon (see Supplementary Materials Table S4 for site details). CWT describes variance as a function of time and frequency, with areas significant (95%) relative to red noise enclosed by solid black line. Color mapping, with the key at right, is spectral power (high variance yellow, low variance blue). The title at top gives the name of the series, whether it was transformed (none were), and the year sequences (relative for floating, absolute for modern). Series smoothed by a low-pass Hamming filter (number of weights and 50% response wavelength annotated) are plotted below CWT. Red vertical bar to the left of CWT marks the approximate range of wavelengths passed by the filter; the percentage of the original variance retained in the smoothed series is annotated in the box in the upper right of the time plot.

Studies of late Quaternary climate variability on high numbers of subfossil tree samples are extremely rare [57–60]. Subfossil wood buried simultaneously by catastrophic events like tephra deposition, flooding, or earthquakes could be considered random tree-

Studies of Late Quaternary climate variability on high numbers of subfossil tree samples are extremely rare [57–60]. Subfossil wood buried simultaneously by catastrophic events like tephra deposition, flooding, or earthquakes could be considered random tree-ring sampling, which contradicts the dendrochronological principal of site and tree selection and which has been used in the tree-ring reconstruction of climate variability [61]. Nevertheless, the multi-parameter approach tested here validates the correspondence of tree-ring responses. Furthermore, the spectral properties of tree-ring parameters from ancient trees make it possible to compare low- and high-frequency variability with modern tree growth with a known climatic response. Although the spatial signature of the ancient tree-ring response to climate change cannot be achieved at such ancient times, the glimpse into the ancient environments and climate variability provides a new perspective on the interpretation of late Quaternary climate change, yet this view is very fragmented and not coherent.

4. Conclusions

Proxy records of climate variability during the late Quaternary are necessary to understand the patterns of climate change on various time scales and their relationships to climate forcing. We explore response of ancient tree-ring proxies of temperature and moisture on annual and decadal scales using macrofossils. An ancient landslide deposit in Oregon, U.S., fortuitously preserved large Douglas fir (*Pseudotsuga menziesii* (Mirb.) Franco) trees. Initial wood radiocarbon ages >40 ka suggested a date in Marine Isotope Stage 3 (MIS 3, ca. 60 to 27 ka), a generally cold interval interrupted by brief Dansgaard–Oeschger warm excursions that might have been favorable to forest establishment or expansion. Subsequent advanced high-precision radiocarbon dating indicated that the age exceeds 62 ka. However, exactly 62 ka would be less likely because it would align with a cold interval in MIS 5a, whereas later MIS 5 substages would have brief warmer intervals more optimal for Douglas fir establishment and growth, particularly the prolonged warm MIS 5e (ca. 120 ka) approximately corresponding to the Eemian interglacial with conditions similar to the current Holocene interglacial period. This discovery provided a remarkable opportunity to assess the environment of that time using tree rings.

In its own right, the development of a robust 297-year tree-ring width chronology from 12 Douglas fir logs indicated some common forcing to growth, which would frequently be interpreted as being related to climate. Because of accurate dating and a sufficient number of tree samples, 227-year reliable records of tree-ring cellulose $\delta^{13}C$ and $\delta^{18}O$ series provided further proxies to understand conditions at the time the trees grew. We could not use standard dendroclimatology techniques comparing tree-ring records with instrumental data. However, we consulted isotope–climate relationships reported in modern coast Douglas fir studies, and we examined correlations among records and their spectral properties. The O-isotopes were strongly correlated with ring widths and may be an indicator of moisture as suggested by modern studies. The detrended C-isotopes do not correlate with O-isotopes, which may indicate that C-isotopes are responding to sunlight or to temperature. Tables S5 and S6 in the Supplementary Materials show various ring width and isotope parameters for modern and ancient coast Douglas fir, which indicate these parameters in the ancient trees fall into the range of values observed in the modern trees. This suggests the environment and tree growth/physiology response was similar 120,000 years ago to that of today in coastal Oregon, at least according to Douglas fir tree rings.

The spectra of ancient as well as modern chronologies are dominated by low frequencies, but significant spectral peaks relative to red noise often appear at high frequencies (wavelengths 2.1–4 years). Wavelet analysis indicates that any cyclic behavior is transient rather than persistent over centuries. The spectral analysis does not indicate any strong, persistent, regular ENSO or PDO periodicities in any of the proxies, and they are not seen in modern coast Douglas fir tree-ring width chronologies, so the implication is that the Eemian Douglas fir growth influences are similar to those of modern.

This is the first case study of MIS 5 tree rings in the North America made from well-replicated fossil tree-ring samples. It should be noted that this tree-ring collection is unique and very unlikely could be replicated due to age uncertainty. With that, we conclude that the application of tree rings for the assessment of the late Quaternary climate at interannual–decadal scales may be difficult, although it would be useful to explore further the potential of tree rings of macrofossils.

Supplementary Materials: The following supporting information can be downloaded at: https://www.mdpi.com/article/10.3390/f13122161/s1, Table S1: Summary of 13 wood specimens; Table S2: Summary of tree-ring width chronology and ring isotope chronologies; Table S3: Results of original AMS radiocarbon dating; Table S4: Site statistics of modern Douglas-fir ring width chronologies [29,30]; Table S5: Statistics of tree-ring width measurements and index chronologies from the ancient and modern Douglas-fir; Table S6: Comparison of mean isotopic composition between modern coast Douglas-fir tree rings and the ancient one [50–53]; Figure S1: The $\delta^{13}C$ (left) and $\delta^{18}O$ (right) time series for the Oregon landslide Douglas-fir; Figure S2: Continuous wavelet transforms (CWT) and smoothed time series plots of modern tree-ring width chronologies.

Author Contributions: Design of the study and funding acquisition: A.J.T.J., I.P.P., S.W.L. and P.V.d.W. Sample acquisition: J.S., N.R.T. and P.V.d.W. Data acquisition: I.P.P., S.W.L. and A.J.T.J. Data analysis and calculations: I.P.P. and D.M.M. Data interpretation of data: I.P.P., S.W.L., D.M.M. and B.A.B. Writing up the manuscript: S.W.L. and I.P.P. All authors have read and agreed to the published version of the manuscript.

Funding: This research was supported by U.S. National Science Foundation (NSF) AGS P2C2 Grant #1103417. Principal Investigators: A.J.T. Jull, S.W. Leavitt, I.P. Panyushkina and P. Van de Water.

Institutional Review Board Statement: Not applicable.

Informed Consent Statement: Not applicable.

Data Availability Statement: The datasets of this study are available by request from corresponding author I. Panyushkina (ipanyush@arizona.edu).

Acknowledgments: We are thankful to research staff at the Laboratory of Tree-ring Research, University of Arizona for helping with the wood processing. Chris Baisan cut the large cross-sections into manageable sizes. Ken LeRoy helped to surface samples, measure ring widths, separate rings, and chemically pretreat samples for isotope analysis. David Dettman and Xiaoyu Zhang of the Dept. of Geosciences at the University of Arizona oversaw the isotope analysis in the Environmental Isotope Laboratory. We thank Julio Betancourt and Cathy Whitlock for sharing thoughts regarding the interpretation of the possible absolute age of the trees. We are grateful to Alan Hogg, University of Waikato, New Zealand, who provided the ultra-high-resolution ages of wood samples. Alex J. Wiedenhoeft, USDA Forest Products Laboratory, Madison, Wisconsin, identified the tree species of subfossil wood. We would be remiss if we did not give a nod to Claude Warren of the Anthropology Department at the University of Nevada, Las Vegas, whose introductory archaeology class was taken by author J.S. in 1980, planting awareness of the potential value of such a discovery to understanding past climate and prompting ODOT's special care and interest. This investigation greatly benefited from ODOT logistical support and technical assistance. This included procuring the initial ^{14}C dates of the first recovered tree trunk, organic matter, and wood fragments appearing in regolith borings taken along the highway route and arranging shipment of the large samples to the University of Arizona.

Conflicts of Interest: The authors declare no conflict of interest that may be perceived as influencing the representation or interpretation of reported research results.

References

1. Kageyama, M.; Braconnot, P.; Harrison, S.P.; Haywood, A.M.; Jungclaus, J.; Otto-Bliesner, B.L.; Peterschmitt, J.-Y.; Abe-Ouchi, A.; Albani, S.; Bartlein, P.J.; et al. PMIP4-CMIP6: The contribution of the Paleoclimate Modelling Intercomparison Project to CMIP6. *Geosci. Model Dev. Discuss.* **2018**, *11*, 1033–1057. [CrossRef]
2. Bradbury, J.P.; Grosjean, M.; Stine, S.; Sylvestre, F. Full and Late Glacial lake records along the PEP1 transect: Their role in developing interhemispheric paleoclimate interactions. In *Interhemispheric Climate Linkages*; Markgraf, V., Ed.; Academic Press: Cambridge, MA, USA, 2001; pp. 265–292.

3. Markgraf, V.; Diaz, H.F. The past ENSO record: A synthesis. In *El Niño and the Southern Oscillation: Multiscale Variability and Global Impacts*; Diaz, H.F., Markgraf, V., Eds.; Cambridge University Press: Cambridge, UK, 2001; pp. 465–488.
4. Labeyrie, L.; Cole, J.; Alverson, K.; Stocker, T. The History of Climate Dynamics in the Late Quaternary. In *Paleoclimate, Global Change and the Future. Global Change—The IGBP Series*; Alverson, K.D., Pedersen, T.F., Bradley, R.S., Eds.; Springer: Berlin/Heidelberg, Germany, 2003. [CrossRef]
5. The Gymnosperm Database. Pseudotsuga Menziesii. Edited by Christopher J. Earle. 2021. Available online: https://www.conifers.org/pi/Pseudotsuga_menziesii.php (accessed on 5 December 2022).
6. Brubaker, L.B. Climate change and the origin of old-growth Douglas-fir forests in the Puget Sound Lowland. In *Wildlife and Vegetation of Unmanaged Douglas-Fir Forests*; Ruggiero, L.F., Aubry, K.B., Carey, A.B., Huff, M.H., Eds.; USDA Forest Service: Washington, DC, USA, 1991; General Technical Report PNW-GTR-285.
7. Gugger, P.F.; Sugita, S. Glacial populations and postglacial migration of Douglas-fir based on fossil pollen and macrofossil evidence. *Quat. Sci. Rev.* **2010**, *29*, 2052–2070. [CrossRef]
8. Bartlein, P.J.; Anderson, K.H.; Anderson, P.M.; Edwards, M.E.; Mock, C.J.; Thompson, R.S.; Webb, R.S.; Whitlock, C. Paleoclimate simulations for North America over the past 21,000 years: Features of the simulated climate and comparisons with paleoenvironmental data. *Quat. Sci. Rev.* **1998**, *17*, 549–585. [CrossRef]
9. Little, E.L.; Viereck, L.A. *Atlas of United States Trees, Volume 1: Conifers and Important Hardwoods*; U.S. Dept. of Agriculture, Forest Service: Washington, DC, USA, 1971.
10. Zhang, Q.-B.; Hebda, R.J. Abrupt climate change and variability in the past four millennia of the southern Vancouver Island, Canada. *Geophys. Res. Lett.* **2005**, *32*, L16708. [CrossRef]
11. de Graauw, K.K.; Towner, R.H.; Grissino-Mayer, H.D.; Kessler, N.V.; Knighton-Wisor, J.; Steffen, A.; Doerner, J.P. Historical dendroarchaeology of two log structures in the Valles Caldera National Preserve, New Mexico, USA. *Dendrochronologia* **2014**, *32*, 336–342. [CrossRef]
12. Klesse, S.; DeRose, R.J.; Babst, F.; Black, B.A.; Anderegg, L.D.L.; Axelson, J.; Ettinger, A.; Griesbauer, H.; Guiterman, C.H.; Harley, G.; et al. Continental-scale tree-ring-based projection of Douglas-fir growth: Testing the limits of space-for-time substitution. *Glob. Change Biol.* **2020**, *26*, 5146–5163. [CrossRef]
13. Balanzategui, D.; Nordhauß, H.; Heinrich, I.; Biondi, F.; Miley, N.; Hurley, A.G.; Ziaco, E. Wood anatomy of Douglas-fir in Eastern Arizona and its relationship with Pacific Basin climate. *Front. Plant Sci.* **2021**, *12*, 1812. [CrossRef]
14. Brookes, W.; Daniels, L.D.; Copes-Gerbitz, K.; Baron, J.N.; Carroll, A.L. A disrupted historical fire regime in central British Columbia. *Front. Ecol. Evol.* **2021**, *9*, 420. [CrossRef]
15. Klamath Inventory and Monitoring Network, 2017. Coast Douglas-fir (Pseudotsuga menziesii menziesii). Klamath Inventory and Monitoring Network Featured Creature, National Park Service, Dept. of Interior, prepared by Linda Mutch. Available online: https://irma.nps.gov/DataStore/DownloadFile/583841 (accessed on 5 December 2022).
16. Tappeiner, J.C.; Huffman, D.; Marshall, D.; Spies, T.A.; Bailey, J.D. Density, ages, and growth rates in old-growth and young-growth forests in coastal Oregon. *Can. J. For. Res.* **1997**, *27*, 638–648. [CrossRef]
17. Hammond, C.M.; Meier, D.; Beckstrand, D. Paleo-landslides in the Tyee Formation and highway construction, central Oregon Coast Range. In *Volcanoes to Vineyards: Geologic Field Trips through the Dynamic Landscape of the Pacific Northwest: Geological Society of America Field Guide*; O'Connor, J.E., Dorsey, R.J., Madin, I.P., Eds.; Geological Society of America: Boulder, CO, USA, 2009; Volume 15, pp. 481–494. [CrossRef]
18. Cornforth Consultants. *Geotechnical Data Report- Phase 2A. Supplemental Geotechnical Investigation*; Pioneer Mountain to Eddyville Section US Route 20 Relocation Design and Construction; Cornforth Consultants, Inc.: Portland, OR, USA, 2008; Available online: https://people.wou.edu/~{}taylors/g322/HWY20_ODOT_Project.pdf (accessed on 10 October 2022).
19. Holmes, R.L. Computer-assisted quality control in tree-ring dating and measurement. *Tree-Ring Bull.* **1983**, *43*, 69–75.
20. Cook, E.R.; Krusic, P.J.; Holmes, R.H.; Peters, K. Program ARSTAN, Version 41d, 2007. Available online: http://www.ldeo.columbia.edu/tree-ring-laboratory (accessed on 10 October 2022).
21. McCarroll, D.; Duffy, J.E.; Loader, N.J.; Young, G.H.; Davies, D.; Miles, D.; Bronk Ramsey, C. Are there enormous age-trends in stable carbon isotope ratios of oak tree rings? *Holocene* **2020**, *30*, 1637–1642. [CrossRef]
22. Leavitt, S.W.; Danzer, S.R. Method for batch processing small wood samples to holocellulose for stable-carbon isotope analysis. *Anal. Chem.* **1993**, *65*, 87–89. [CrossRef]
23. Panyushkina, I.P.; Leavitt, S.W.; Thompson, T.A.; Schneider, A.F.; Lange, T. Environment and paleoecology of a 12 ka mid-North American Younger Dryas forest chronicled in tree rings. *Quat. Res.* **2008**, *70*, 433–441. [CrossRef]
24. Sternberg, L.S.L. Oxygen and hydrogen isotope measurements in plant cellulose analysis. In *Plant Fibres. Modern Methods of Plant Analysis V*; Linskens, H.F., Jackson, J.F., Eds.; Springer: New York, NY, USA, 1989; pp. 1089–1099.
25. Bloomfield, P. *Fourier Analysis of Time Series: An Introduction*; Wiley: New York, NY, USA, 2000.
26. Torrence, C.; Compo, G.P. A practical guide to wavelet analysis. *Bull. Am. Meteorol. Soc.* **1998**, *79*, 61–78. [CrossRef]
27. Grinsted, A.; Moore, J.C.; Jevrejeva, S. Application of cross wavelet transform and wavelet coherence to geophysical time series. *Nonlinear Process. Geophys.* **2004**, *11*, 561–566. [CrossRef]
28. Chatfield, C. *The Analysis of Time Series: An Introduction*; Chapman and Hall/CRC Press: Boca Raton, FL, USA, 2004.

29. Black, B.A.; Dunham, J.B.; Blundon, B.W.; Brim-Box, J.; Tepley, A.J. Long-term growth-increment chronologies reveal diverse influences of climate forcing on freshwater and forest biota in the Pacific Northwest. *Glob. Change Biol.* **2015**, *21*, 594–604. [CrossRef]
30. Dziak, R.P.; Black, B.A.; Wei, Y.; Merle, S.G. Assessing local impacts of the 1700 CE Cascadia earthquake and tsunami using tree-ring growth histories: A case study in South Beach, Oregon, USA. *Nat. Hazards Earth Syst. Sci.* **2021**, *21*, 1971–1982. [CrossRef]
31. Kudsk, S.; Olsen, J.; Hodgins, G.; Molnár, M.; Lange, T.; Nordby, J.; Jull, A.J.T.; Varga, T.; Karoff, C.; Knudsen, M. An intercomparison project on 14C from single-year tree rings. *Radiocarbon* **2021**, *63*, 1445–1452. [CrossRef]
32. Slota, P.J.; Jull, A.J.T.; Linick, T.W.; Toolin, L.J. Preparation of small samples for 14C accelerator targets by catalytic reduction of CO. *Radiocarbon* **1987**, *29*, 303–306. [CrossRef]
33. Pigati, J.S.; Quade, J.; Wilson, J.; Jull AJ, T.; Lifton, N.A. Development of a low-level vacuum extraction system for 14C dating of old (40–60ka) samples. *Quat. Int.* **2007**, *166*, 4–14. [CrossRef]
34. Hogg, A.G.; Lowe, D.J.; Hendy, C.H. University of Waikato radiocarbon dates I. *Radiocarbon* **1987**, *29*, 263–301. [CrossRef]
35. Stuiver, M.; Polach, H. Discussion: Reporting of 14C data. *Radiocarbon* **1977**, *19*, 355–363. [CrossRef]
36. McCarroll, D.; Loader, N.J. Stable isotopes in tree rings. *Quat. Sci. Rev.* **2004**, *23*, 771–801. [CrossRef]
37. Leavitt, S.W. Tree-ring C-H-O isotope variability and sampling. *Sci. Total Environ.* **2010**, *408*, 5244–5253. [CrossRef]
38. Imbrie, J.; Hays, J.D.; McIntyre, A.; Mix, A.C.; Morley, J.J.; Pisias, N.G.; Prell, W.L.; Shackleton, N.J. The orbital theory of Pleistocene climate: Support from a revised chronology of the marine $\delta^{18}O$ record. In *Milankovitch and Climate*; Berger, A., Imbrie, J., Hays, J., Kukla, G.J., Saltzman, E., Eds.; D. Reidel Publishing: Boston, MA, USA, 1984; pp. 269–305.
39. van Meerbeeck, C.J.; Renssen, H.; Roche, D.M. How did Marine Isotope Stage 3 and Last Glacial Maximum climates differ? Perspectives from equilibrium simulations. *Clim. Past* **2009**, *5*, 33–51. [CrossRef]
40. Hart, R.; Peterson, C. Episodically buried forests in the Oregon surf zone. *Or. Geol.* **1997**, *59*, 131–144.
41. Smyth, W.D.; Hart, R.A.; Reimer, P.J. Pleistocene Forests preserved in Oregon coast sediments. *Eos Trans. Am. Geophys. Union* **2005**, *86*, 2–3. [CrossRef]
42. Railsback, L.B.; Gibbard, P.L.; Head, M.J.; Voarintsoa, N.R.G.; Toucanne, S. An optimized scheme of lettered marine isotope substages for the last 1.0 million years, and the climatostratigraphic nature of isotope stages and substages. *Quat. Sci. Rev.* **2015**, *111*, 94–106. [CrossRef]
43. Shin, J.; Nehrbass-Ahles, C.; Grilli, R.; Chowdhry Beeman, J.; Parrenin, F.; Teste, G.; Landais, A.; Schmidely, L.; Silva, L.; Schmitt, J.; et al. Millennial-scale atmospheric CO_2 variations during the Marine Isotope Stage 6 period (190–135 ka). *Clim. Past* **2020**, *16*, 2203–2219. [CrossRef]
44. Shackleton, N.J.; Sánchez-Goñi, M.F.; Pailler, D.; Lancelot, Y. Marine Isotope Substage 5e and the Eemian Interglacial. *Glob. Planet. Change* **2003**, *36*, 151–155. [CrossRef]
45. González-Elizondo, M.; Jurado, E.; Návar, J.; González-Elizondo, M.C.; Villanueva, J.; Aguirre, O.; Jiménez, J. Tree-rings and climate relationships for Douglas-fir chronologies from the Sierra Madre Occidental, Mexico: A 1681–2001 rain reconstruction. *For. Ecol. Manag.* **2005**, *213*, 39–53. [CrossRef]
46. Griffin, D.; Meko, D.M.; Touchan, R.; Leavitt, S.W.; Woodhouse, C.A. Latewood chronology development for summer-moisture reconstruction in the U.S. Southwest. *Tree-Ring Res.* **2011**, *67*, 87–101. [CrossRef]
47. Griffin, D.; Woodhouse, C.A.; Meko, D.M.; Stahle, D.W.; Faulstich, H.L.; Carrillo, C.; Touchan, R.; Castro, C.L.; Leavitt, S.W. North American monsoon precipitation reconstructed from tree-ring latewood. *Geophys. Res. Lett.* **2013**, *40*, 954–958. [CrossRef]
48. Restaino, C.M.; Peterson, D.L.; Littell, J. Douglas fir growth decreases with drought. *Proc. Natl. Acad. Sci. USA* **2016**, *113*, 9557–9562. [CrossRef]
49. Rebetz, M.; Saurer, M.; Cherubini, P. To what extent can oxygen isotopes in tree rings and precipitation be used to reconstruct past atmospheric temperature? A case study. *Clim. Change* **2003**, *61*, 237–248. [CrossRef]
50. Panek, J.A.; Waring, R.H. Stable carbon isotopes as indicators of limitations to forest growth imposed by climate stress. *Ecol. Appl.* **1997**, *7*, 854–863. [CrossRef]
51. Lévesque, M.; Saurer, M.; Siegwolf, R.; Eilmann, B.; Brang, P.; Bugmann, H.; Rigling, A. Drought response of five conifer species under contrasting water availability suggests high vulnerability of Norway spruce and European larch. *Glob. Change Biol.* **2013**, *19*, 3184–3199. [CrossRef]
52. Roden, J.S.; Bowling, D.R.; McDowell, N.G.; Bond, B.J.; Ehleringer, J.R. Carbon and oxygen isotope ratios of tree ring cellulose along a precipitation transect in Oregon, United States. *J. Geophys. Res.* **2005**, *110*, G02003. [CrossRef]
53. Barnard, H.R.; Brooks, J.R.; Bond, B.A. Applying the dual-isotope conceptual model to interpret physiological trends under uncontrolled conditions. *Tree Physiol.* **2012**, *32*, 1183–1198. [CrossRef]
54. Lee, E.H.; Beedlow, P.A.; Brooks, J.R.; Tingey, D.T.; Wickham, C.; Rugh, W. Physiological responses of Douglas-fir to climate and forest disturbances as detected by cellulosic carbon and oxygen isotope ratios. *Tree Physiol.* **2021**, *42*, 5–25. [CrossRef]
55. Lee, E.H.; Beedlow, P.A.; Waschmann, R.S.; Cline, S.; Bollman, M.; Wickham, C.; Testa, N. Tree-ring history of Swiss needle cast impact on Douglas-fir growth in Western Oregon: Correlations with climatic variables. *J. Plant Sci. Phytopathol.* **2021**, *5*, 76–87.
56. Stahle, D.W.; Burnette, D.J.; Villanueva, J.; Cerano, J.; Fye, F.K.; Griffin, R.D.; Cleaveland, M.K.; Stahle, D.K.; Edmondson, J.R.; Wolff, K.P. Tree-ring analysis of ancient baldcypress trees and subfossil wood. *Quat. Sci. Rev.* **2012**, *34*, 1–15. [CrossRef]
57. Roig FALe-Quesne, C.; Boninsegna, J.A.; Briffa, K.R.; Lara, A.; Grudd, H.; Jones, P.D.; Villagrán, C. Climate variability 50,000 years ago in mid-latitude Chile as reconstructed from tree rings. *Nature* **2001**, *410*, 567–570. [CrossRef]

58. Leavitt, S.W.; Panyushkina, I.P.; Lange, T.; Wiedenhoeft, A.; Cheng, L.; Hunter, R.D.; Hughes, J.; Pranschke, F.; Schneider, A.F.; Moran, J.; et al. Climate in the Great Lakes region between 14,000 and 4000 years ago from isotopic composition of conifer wood. *Radiocarbon* **2006**, *48*, 205–217. [CrossRef]
59. Panyushkina, I.P.; Leavitt, S.W. Ancient boreal forests under the environmental instability of the glacial to post-glacial transition in the Great Lakes region (14,000–11,000 years BP). *Can. J. For. Res.* **2013**, *43*, 1032–1039. [CrossRef]
60. Reinig, F.; Nievergelt, D.; Esper, J.; Friedrich, M.; Helle, G.; Hellmann, L.; Kromer, B.; Morganti, S.; Pauly, M.; Sookdeo, A.; et al. New tree-ring evidence for the Late Glacial period from the northern pre-Alps in eastern Switzerland. *Quat. Sci. Rev.* **2019**, *186*, 215–224. [CrossRef]
61. Fritts, H.C. *Tree Rings and Climate. London, New York and San Francisco*; Academic Press: Cambridge, MA, USA, 1976; 567p.